

Controllable Image Restoration for Under-Display Camera in Smartphones

Supplementary Material

Kinam Kwon* Eunhee Kang* Sangwon Lee Su-Jin Lee Hyong-Euk Lee
ByungIn Yoo Jae-Joon Han
Samsung Advanced Institute of Technology (SAIT), South Korea

We provide more details of dataset and experimental results in this supplementary material. In detail, we provide the detailed description of aligned monitor-captured dataset in [Section 1](#). [Section 2](#) shows the effect of the proposed multi-dilated block. [Section 3](#) shows simultaneous controllability with deblurring and denoising. Finally, high-resolution restored images are provided in [Section 4](#).

1. Aligned dataset

Aligned images were collected by smartphones (Samsung Galaxy S20 Plus) under on-device 3A conditions. The images were 10-bit Bayer-pattern 4032×3024 linear-RGB images. The images were labeled as UDC images and non-UDC images, depending on whether there was a panel in front of the camera when the relevant image was captured. We utilized a monitor-camera imaging system [5] to collect aligned images for quantitative evaluation. DIV2k images [2] displayed on a 4k monitor were captured by the smartphone. Non-UDC images were captured 16 times to generate a noiseless non-UDC image as in [1]. The noiseless non-UDC image was registered with the corresponding UDC image by matching SURF [3] features and estimating projective transforms. The registered non-UDC image was normalized channel-wise to compensate for the wavelength-dependent transmission rate of the UDC image. The UDC image and corresponding registered non-UDC image were utilized as the input and targeted output. Data with moire/flicker artifacts or unsatisfactory registration regions were screened out. Finally, 300 pairs were collected and split into 200 for training (only for the Real-mon), 60 for validation, and 40 for testing. [Fig. 1](#) shows samples of the collected aligned dataset.

2. Effect of multi-dilated block

[Fig. 2](#) showed the restored images depending on the network architectures for noise estimator. Compared noise estimators are based on EDSR [4]. Each noise estimator consists of the conventional residual blocks or the proposed

multi-dilated (MD) blocks, and the number of the blocks is 3 or 6. They are labeled as “Res3”, “MD3”, “Res6”, and “MD6”. Their receptive fields are, 17×17 , 29×29 , 29×29 , and 53×53 , and the numbers of their weights are 57.8k, 57.8k, 113.4k, and 113.4k, respectively. The larger the receptive field and the number of weights are, the better the results are, as shown in [Fig. 2](#). The displayed image size is 260×260 , and the noise estimators with smaller receptive fields than the size of the thin stripe pattern could not discern noise and complex patterns, which results in loss of fine details. The MD block efficiently enlarges the receptive field without increasing the number of weights, which enables the quality improvement in delicate structures.

3. Two-dimensional controllability

[Fig. 3](#) and [Fig. 4](#) show that the proposed method can control denoising and deblurring levels simultaneously. Denoising and deblurring effects are controlled by a noise-balancing level s and kernel representation parameters $k = (b_1, x_1, y_1, x_2, y_2, r_1, r_2)$, respectively. b_1 is the width of main lobe which is related to the sharpness of the restored image. Both s and b_1 levels are controlled to describe the denoising and sharpening effects. In each row of [Fig. 3](#) and [Fig. 4](#), we changed b_1 with fixed s and results are getting sharper as it goes to the right side. Otherwise, in each column of [Fig. 3](#) and [Fig. 4](#), we changed s with fixed b_1 and results are getting smoother as it goes down. The proposed method can produce various restored images by controlling the denoising and sharpening levels, which can be utilized to reflect the user preferences.

4. High-resolution results

The restored images from several methods are displayed at high resolution in [Fig. 5](#), [Fig. 6](#), and [Fig. 7](#). Since the original image size is too large (2736×3648), we display cropped image of size 684×912 at proper location. Also, CGLS consistently shows conceptually and qualitatively better results than WF, we omit the results of WF for better visualization. The denoising and deblurring per-

*These two authors contributed equally.

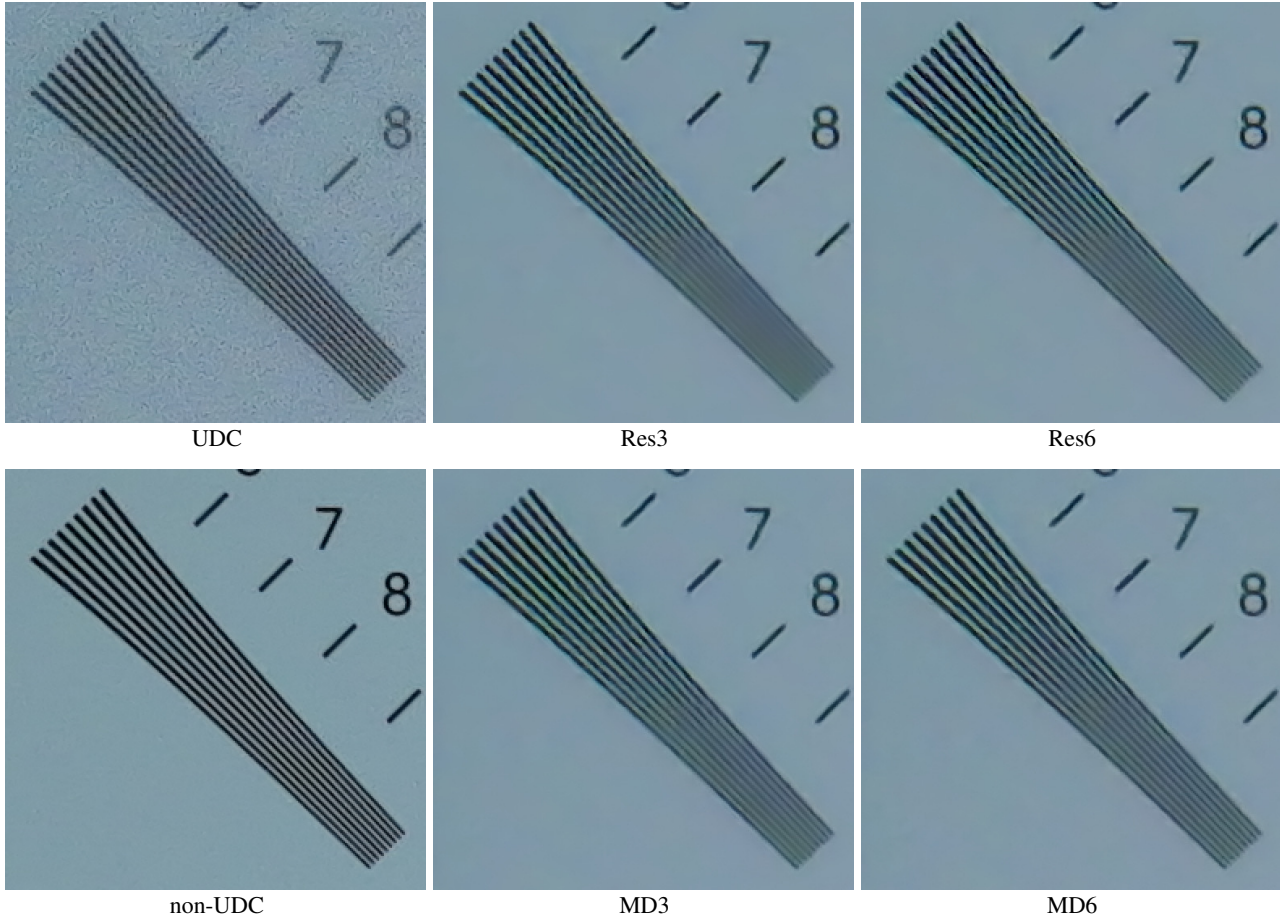


Figure 2: Comparison of residual blocks and MD blocks.

- [3] Herbert Bay, Andreas Ess, Tinne Tuytelaars, and Luc Van Gool. Speeded-up robust features (surf). *Computer vision and image understanding*, 110(3):346–359, 2008. [1](#)
- [4] Bee Lim, Sanghyun Son, Heewon Kim, Seungjun Nah, and Kyoung Mu Lee. Enhanced deep residual networks for single image super-resolution. In *Proceedings of the IEEE conference on computer vision and pattern recognition workshops*, pages 136–144, 2017. [1](#)
- [5] Yuqian Zhou, Michael Kwan, Kyle Tolentino, Neil Emerton, Sehoon Lim, Tim Large, Lijiang Fu, Zhihong Pan, Baopu Li, Qirui Yang, et al. Udc 2020 challenge on image restoration of under-display camera: Methods and results. *arXiv preprint arXiv:2008.07742*, 2020. [1](#)

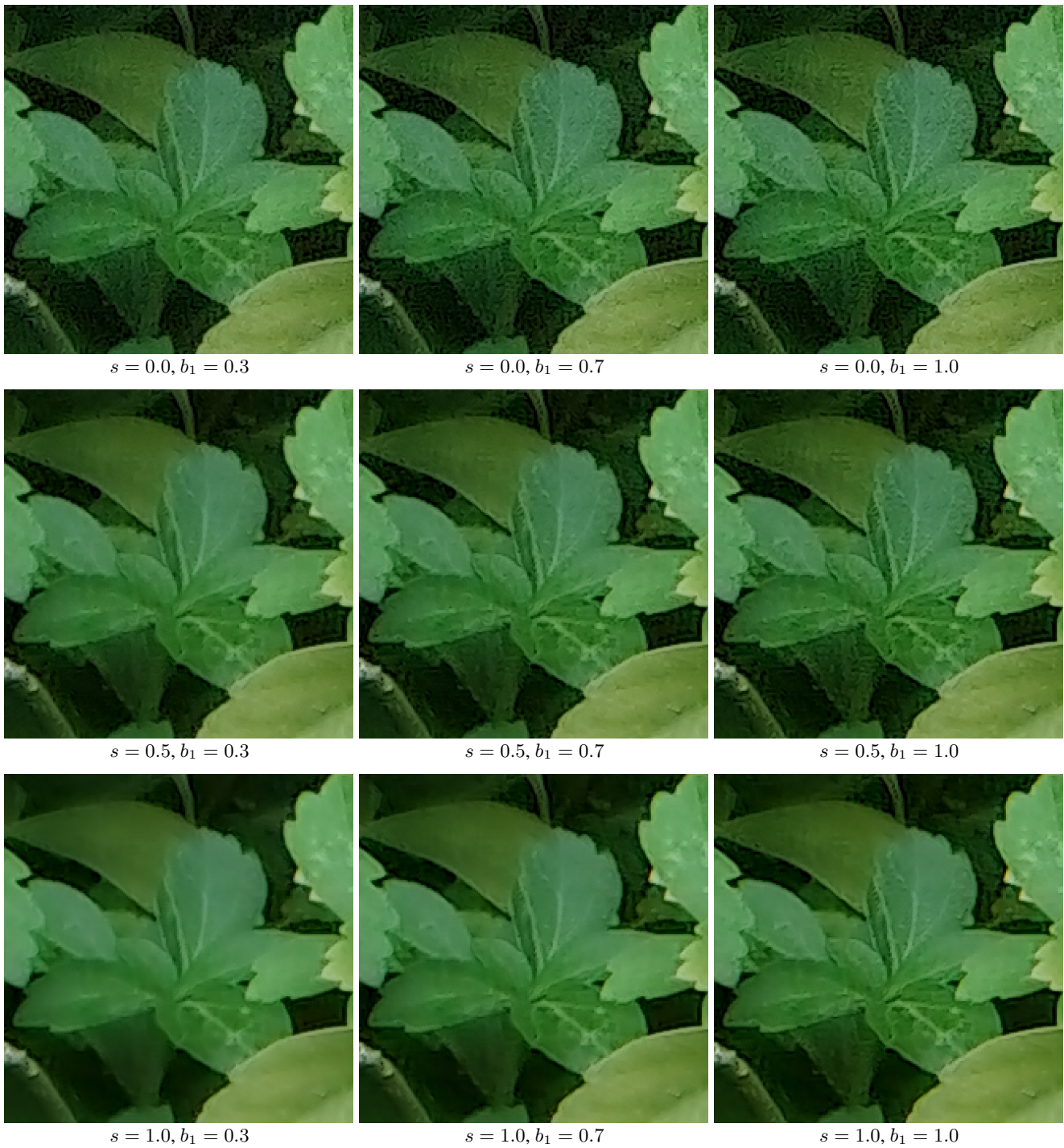


Figure 3: Ours restoration results obtained by controlling noise-balancing level s and width b_1 on an outdoor image.

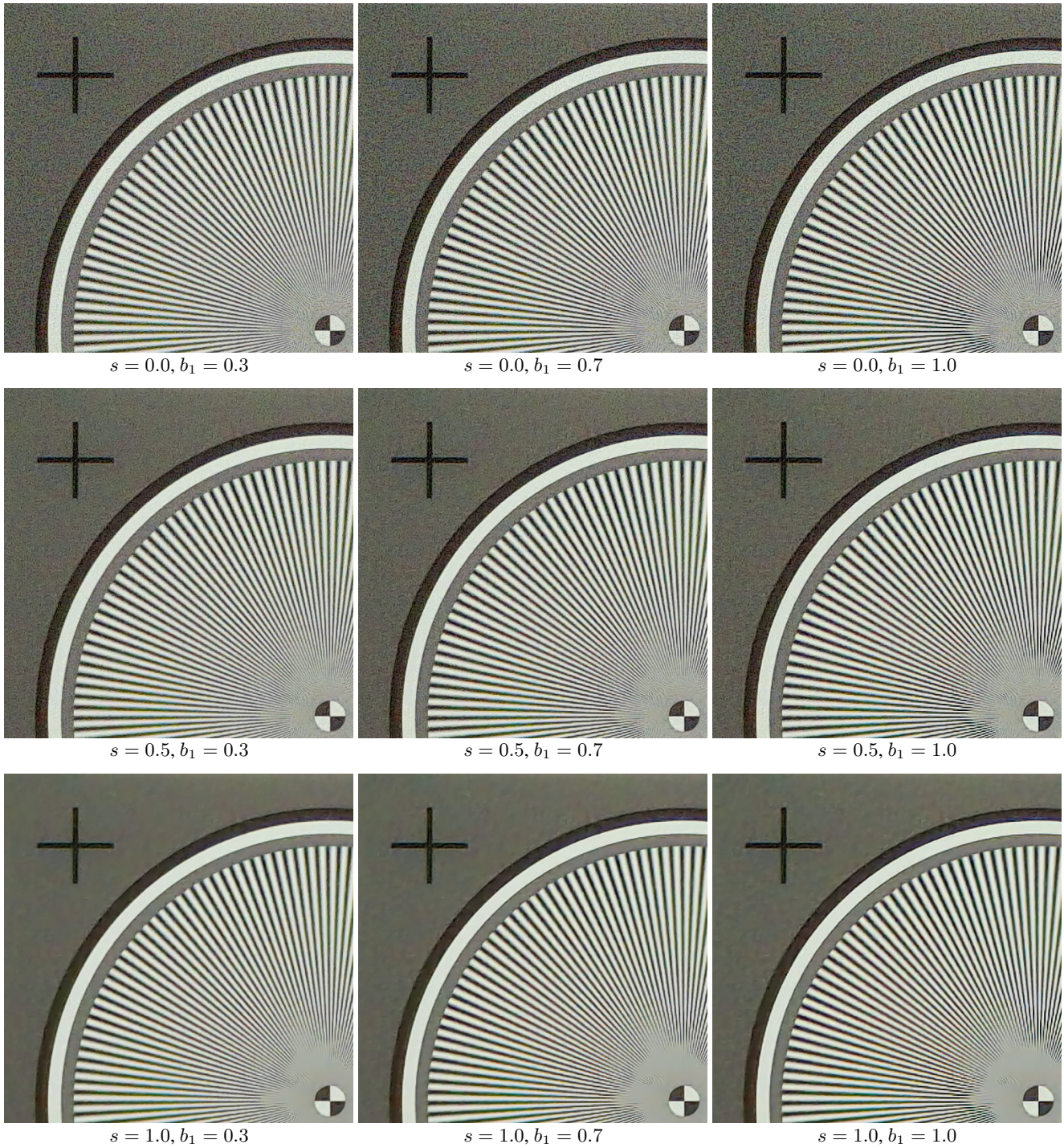


Figure 4: Ours restoration results obtained by controlling noise-balancing level s and width b_1 on a TE42v2 chart image.



UDC



CGLS



Real-mon



Syn-nor



Ours



non-UDC

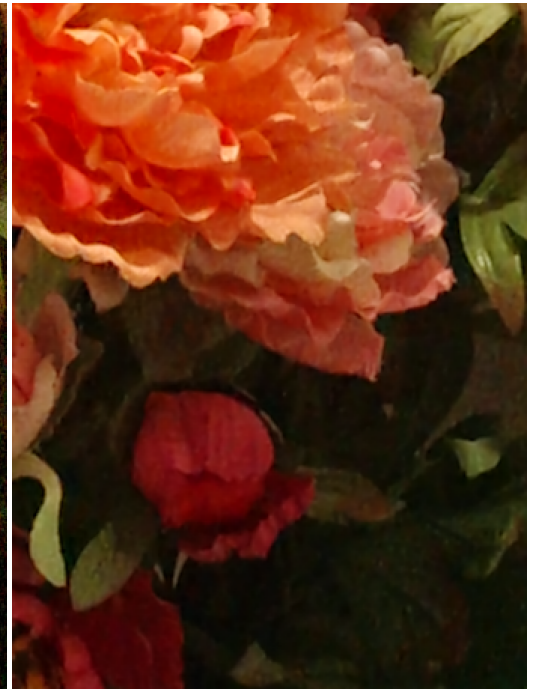
Figure 5: Restoration results obtained using several methods on an outdoor image in daylight.



UDC



CGLS



Real-mon



Syn-nor



Ours



non-UDC

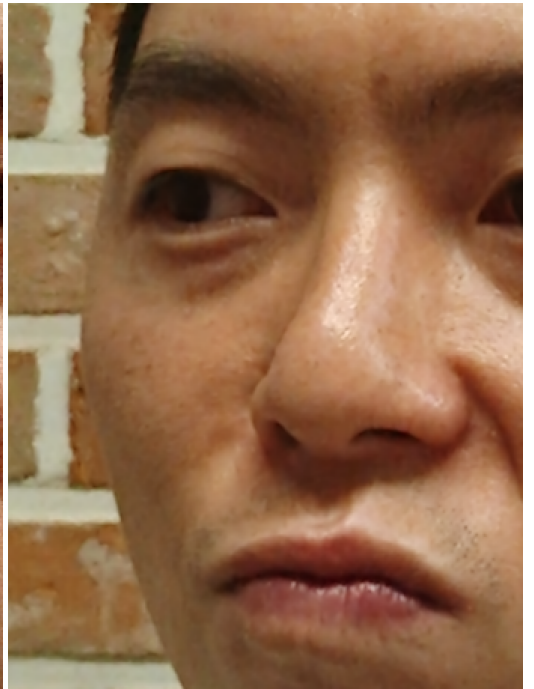
Figure 6: Restoration results obtained using several methods on an indoor image in low-light conditions.



UDC



CGLS



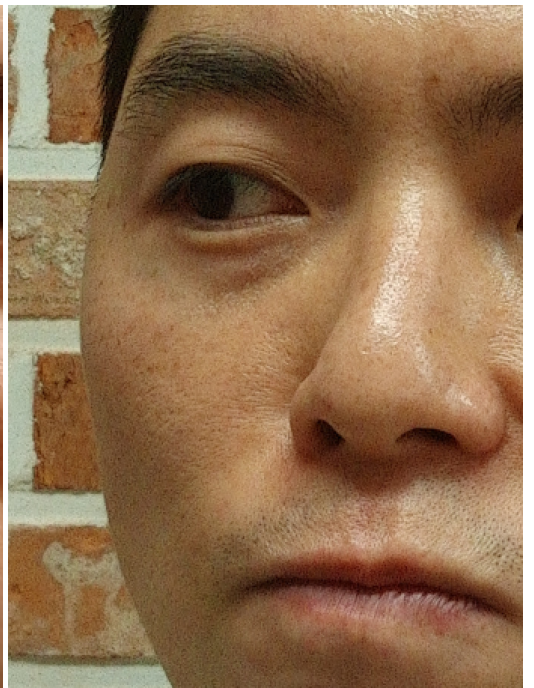
Real-mon



Syn-nor



Ours



non-UDC

Figure 7: Restoration results obtained using several methods on a selfie image in high-light conditions.